ZPS1: zinc starvation for drug sensitivity in *S. cerevisiae*?

Daniel Sumner Magruder & Mary Miller
From the Genetics Course of Dr. Mary Miller, Rhodes College, Memphis TN, 38112

Abstract:

Cancer remains one of the hardest diseases to treat due to its rapid acquirement of resistance as well as treatment options limited to the technology of the time. Out of the fairly successful line of platinum based anti-cancer agents came the promise of ruthenium based drugs with less side effects. Remarkably, ruthenium agents have demonstrated efficacy against drug resistant cell lines lending heavy inquiry as to how these drugs do so. One such agent, KP1019, represses putative zincophore *ZPS1* as well as many other genes regulated by the zinc sensitive transcription factor *ZAP1* as shown by microarray. Perhaps coincidentally, the two main transcription factors responsible for drug efflux mechanisms in yeast require zinc for functionality, thus posing the question if KP1019 staves off resistance by inducing zinc starvation. Here we analyze the affect of KP1019 on *ZPS1*Δ yeast via a budding index and viability assay to see if such a zinc starvation technique both implemented by KP1019 and consequence of *ZPS1* to retain efficacy against drug resistant cell lines. Our results are neutrally inconclusive.

Introduction

Dysregulation of cellular proliferation stems from aberrant signals (conveying growth, division, apoptosis, etc. due to mutated genes) results in cancer (Weinberg, 1996). Life's compounded complexity requires genome wide analysis of a simple model organism to even begin expounding the interactions of these deviant genes. *Saccharomyces cerevisiae* (yeast) host multiple advantageous properties. Namely these are the development of genetics techniques like homologous recombination; counterparts to near half of human disease generating genes and the ability for human protein expression; living succinctly while proving economical; and the complete identification of coding regions within their unadorned genome (Foury, 1997; Goffeau et al., 1996 as in Menacho-Márquez and Murguía, 2007; Menacho-Márquez and Murguía, 2007).

Cellular mechanics in yeast serve to clarify how these pathways can go awry and for relevant breadth analysis for novel treatment strategies, as those mechanisms most fundamental to sustaining life are highly conserved (Menacho-Márquez and Murguía, 2007). Comparative gene expression profiles to drug exposure via microarrays aids in identifying mechanisms of action by unveiling altered gene expressions (Lyons et al., 2000; Menacho-Márquez and Murguía, 2007; NCBI, 2004). If the genes with altered expression have known function, then the mechanism of action can be pieced together via the Saccharomyces Genome Database (SGD) (SGD, 2015).

Currently Ruthenium(Ru)-based chemotherapeutics draw attention due to both potential lower toxicity

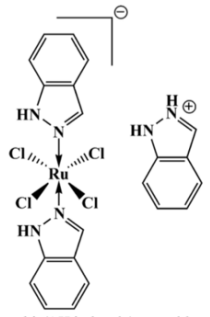

Indazolium-*trans*-bis(1*H*-indazole)-tetrachlororuthenate

Figure 1: Chemical structure of KP1019. Adapted from Antonarakis & Emadi (2010).

Corresponding Author: Magds-16@rhodes.edu

Thanks to the Genome Consortium for Active Teaching for making microarrays accessible, Dr. Mary Miller for the support and guidance outside of and throughout this project, and Dr. Duncan Wilson for the collaborative insight of orthologs in *C. albicans*.

and preferential accumulation in malignant tissues (Sava et al., 1984 as in Antonarakis and Emadi, 2010). Mimicking iron, Ru reaches up to 12-fold concentration in neoplastic cells compared to control via Ru-transferrin complexes as transferrin receptors are up-regulated in cancerous tissues to meet their increased iron need for division (Kratz and Messori, 1993 as in Antonarakis and Emadi, 2010; Sava and Bergamo, 2000 as in Antonarakis and Emadi, 2010; Antonarakis and Emadi, 2010). Heightened metabolic needs and consequently low oxygen environment of neoplastic tissue reduce the fairly inert Ru(III) to active Ru(II), allowing for administration of Ru(III) to preferentially affect malignant cells once a redox reaction occurs (Baitalik and Adhikary, 1997; Chakravarty and Bhattacharya, 1996; Schluga et al., 2006).

Of particular interest is the Ru based drug KP1019, [InH][*trans*-$RuCl_4(In)_2$] (In = indazole), due to its efficacy on cancerous cells that have demonstrated multitudes of resistance (Fig. 1)(Hartinger et al., 2006; Heffeter et al., 2005, 2008). In a clinical trial five out of six patients with advanced cancers achieved stability even when given the minimal dose, noteworthy as KP1019's solubility limits dosage despite linear pharmacokinetics (Hartinger et al., 2006; Heffeter et al., 2008; Stevens et al., 2013). KP1019 activates apoptosis via electron transport chain interference, caspase-3 activation, and bcl-2 inactivation; interestingly, although genotoxic and a weak topoisomerase II poison, KP1019 appears to induce apoptosis without DNA strand breaks (Heffeter et al., 2005; Kapitza et al., 2005a, 2005b as in Antonarakis & Emadi 2010; Stevens et al., 2013). Thus of particular interest are the ramifications of KP1019's iron mimicry (for internalization).

Notably, iron and zinc homeostases are strongly linked. Iron starvation effects the expression of the main zinc transporters and exacerbates zinc toxicity by up-regulation of low affinity iron importers which also pass zinc (Pagani et al., 2007; Yasmin et al., 2009). Mutant screens for zinc sensitive strains of yeast revealed that most had a defect in high affinity iron transportation, thus requiring use of low affinity transporters (Pagani et al., 2007). Further excess zinc has been shown to decrease iron concentrations, demonstrating reciprocity and suggesting iron starvation as the main deleterious affect. Deletion of a major iron homeostasis transcription factor (TF), *AFT1*, results in severe zinc sensitivity *not* resultant of excess intracellular zinc (Pagani et al., 2007). Interestingly a third of genes induced by excessive zinc have promoter sites for the *AFT1* TF (Pagani et al., 2007). Thus the affect of zinc disturbances are of interest.

Both an essential nutrient and oxidatively inert, zinc serves as cofactor for a myriad of proteins – 9% in eukaryotes, 2% specifically for yeast (Citiulo et al., 2012; Crawford and Wilson, 2015; Lyons et al., 2000; Simm et al., 2007; Wilson et al., 2012). Of particular interest are the zinc finger transcription factors Pdr1 and Pdr3. Pleiotropic drug resistance (PDR) is analogous of multidrug resistant (MDR) cell lines. Pdr1&3 promote effective drug efflux systems like ABC transporters and mutations of *PDR1* were hypersensitive to KP1019 (Stevens et al., 2013). Theoretically, zinc starvation could render Pdr1&3 defunct without their zinc cofactors thereby generating an interest in zinc starved situations with drug exposure.

Zinc starvation altered expression in 15% of the genes in the yeast genome, 46 genes may be directly dependent on Zap1p; namely *ZRT1-3*, *ZRC1*, *ZPS1*, & *FET4* (Crawford and Wilson, 2015; Lyons et al., 2000; Simm et al., 2007; Wilson, 2015; Wilson et al., 2012). Fig. 2 provides an overview of zinc homeostasis. *S. cerevisiae's* fungal vacuole, when zinc-sated, can provide zinc for 200 progeny demonstrating the robustness of yeast's zinc acquisition system (Crawford and Wilson, 2015; Simm et al., 2007; Wilson, 2015).

Work with Zps1's *Candida albicans* ortholog Pra1 has revealed this evolutionary successful, fungally conserved, adaption known as a "zincophore" system (Citiulo et al., 2012; Wilson, 2015). A zincophore system contains a secreted zinc-binding scavenger acting with a zinc transporter such as the protein product of *ZRT1* (Citiulo et al., 2012; Wilson, 2015). Of those fungal species having a zincophore systems or analogous bacterial ABC transport systems, most developed synteny – a co-regulated zinc acquisition locus - with the scavenger and transporter (Citiulo et al., 2012). The only putative gene encoding a zincophore identified in *S. cerevisiae*, *ZPS1*, happens to be repressed by KP1019. It is tempting to propose

that repression of *ZPS1* by KP1019 hinders yeast drug efflux systems.

The objective of our study is thus to elucidate whether *ZPS1* plays a pivotal role in KP1019's effectiveness against MDRs. To this extent, we employ microarray technology to invoke comparative gene expression profiling of KP1019 action in yeast and identified *ZPS1* as one of the top 20 most repressed genes by KP1019. Subsequently, KP1019 was introduced to *ZPS1Δ* mutants in both viability and cell cycle arrest assays. If our hypothesis of *ZPS1* repression resulting in Pdr1&3 cofactor starvation and subsequent ineffective drug efflux mechanisms, then it follows viability will be reduced. We predict that *ZPS1Δ* will have no affect on the cell cycle arrest assay, as the gene *ZPS1* is nonessential. Morphology and viability assays did not provide conclusive evidence in regards to our hypothesis . Subsequent work would then need to determine intracellular zinc concentration.

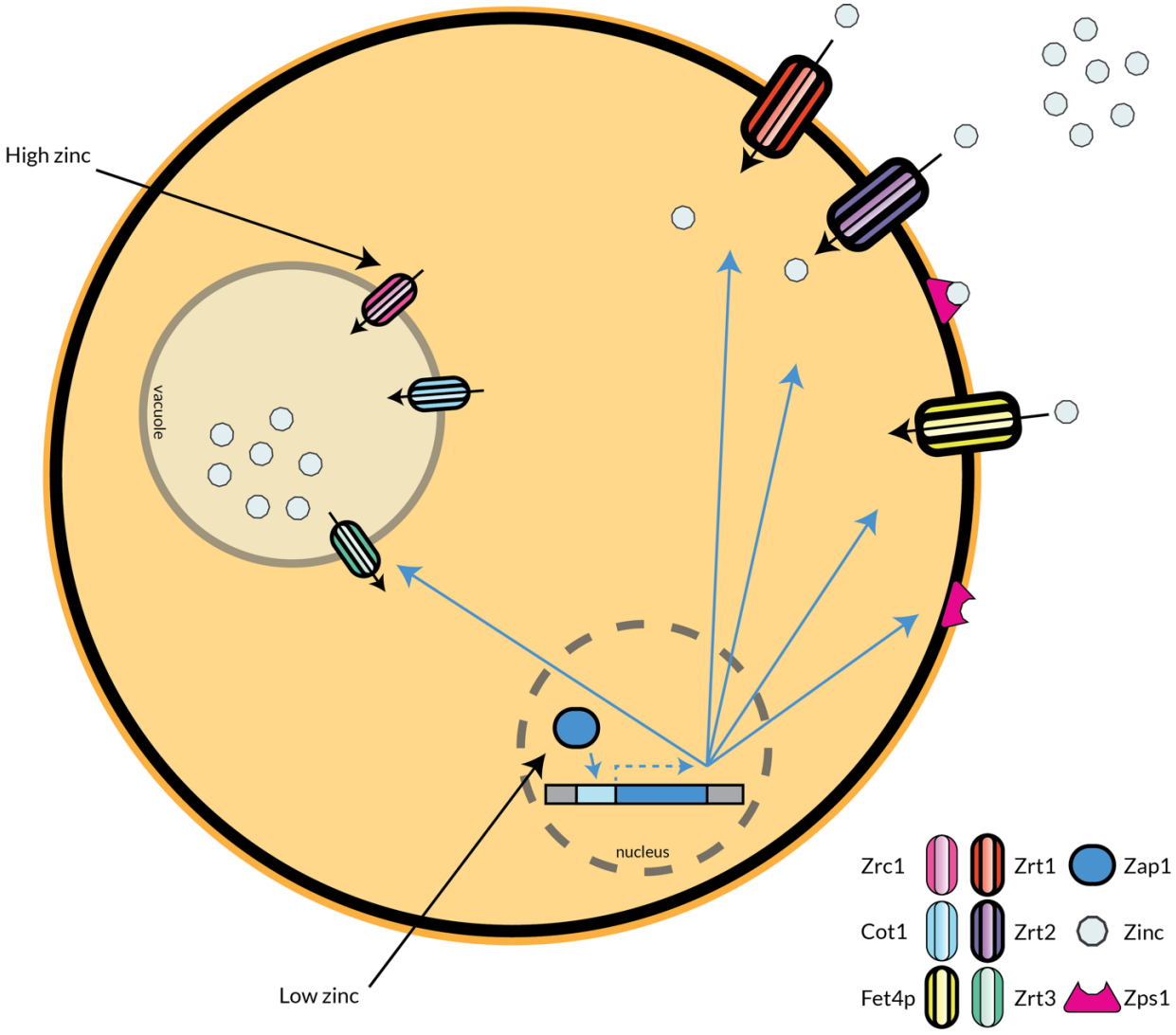

Figure 2: Model of zinc homeostasis in *S. cerevisiae* adapted from Crawford and Wilson (2015). Extracellular zinc importers (Zrt1 & Zrt2) and vacuolar zinc exporter (Zrt3) expression induced by low zinc concentration via zinc-regulated transcription factor (Zap1). Vacuolar zinc importers (Zrc1 & Cot1) serve to detoxify the cell in the presence of heightened zinc concentrations via vacuolar sequestration. Low affinity iron importer (Fet4p) induced by scarce zinc concentrations (via Zap1) demonstartes propensitity to import zinc; also induced by iron starvation, Fet4p leads to zinc sensitivity. Putative GPI-anchored protein and candidate zincophore (Zps1) induced by Zap1 during zinc starvation may serve as a zinc scavenger. *COT1* is paralogous to *ZRC1*.

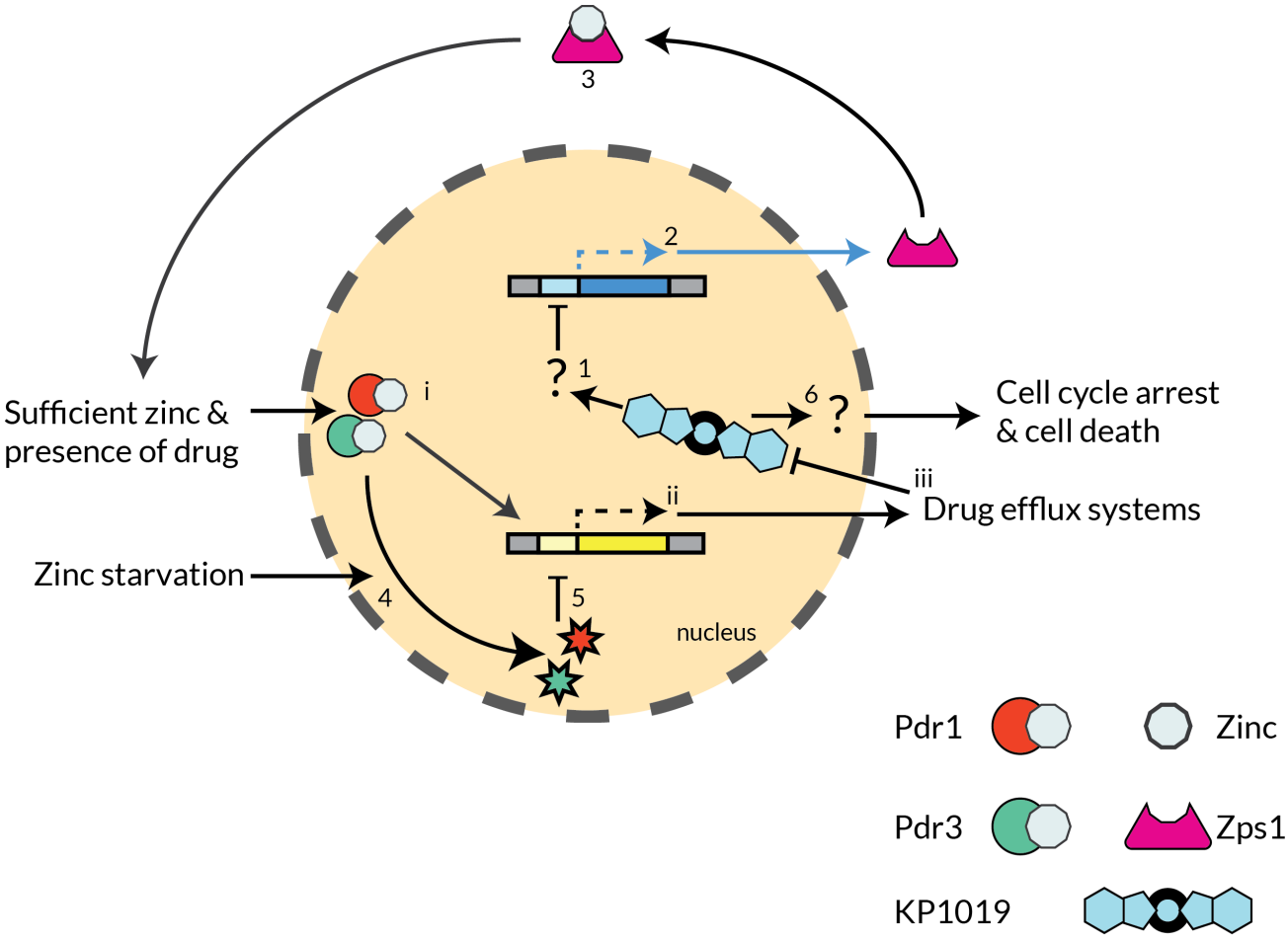

Figure 3: Abridged method of pleiotropic drug resistance. i.) Under the presence of drug and sufficient zinc, zinc finger transcription factors Pdr1 and Pdr3 are activated. ii.) Pdr1 and Pdr3 promote transcription of the drug efflux system. iii.) The expressed drug efflux system attenuates the effect of the drug by removing it from the system. **Proposed KP1019 mechanism of efficacy.** 1.) KP1019 represses expression of the *ZPS1* gene via an unknown pathway. 2.) Repression of the *ZPS1* gene may reduce the expression of the Zps1 protein. 3.) Reduced Zps1 expression would reduce zinc scavenging. 4.) Zinc starvation would deprive Pdr1 and Pdr3 of their zinc cofactors rendering them inactive. 5.) Dsyfunctional Pdr1 and Pdr3 prevent expression of the drug efflux system, hindering efflux of KP1019 from the cell. 6.) Extended exposure to KP1019 allows for cellular arrest and cell death via unknown mechanisms.

Methods

Yeast Strains and Growth Conditions

All yeast strains were obtained from P. Hanson (Birmingham Southern College) or Open Biosystems (Fisher Scientific Incorporated) and were grown using standard growth conditions (Sherman et al, 1989). Cultures were grown in synthetic complete (SC) media at 30°C.

Drug Confirmation

A new batch of KP1019 obtained from Dr. Miller's collaborator was used for this experiment. To confirm quality of the drug, viability and morphology assays included a *RAD9*Δ strain. Previous work has demonstrated that *RAD9*Δ displays a profound phenotype to KP1019, which was observed in both the viability and morphology assays thereby confirming this drug batch's quality (morphological data not shown).

Microarray

Halved (untreated/ treated with 80 µg/mL KP1019 for three hours) samples of log phase strain MMY318-1A (M. Miller) were pelleted and suspended in 250 µL RNAlater (Qiagen RNeasy Kit, catalog number 74104), then stored at -80˚C.

RNA from thawed samples were isolated using the RNAeasy Mini Kit (Qiagen RNeasy Kit, catalog number 74104). Note: cells were lysed enzymatically using Buffer Y1+Zymolyase. Spectrophotometer absorbance readings using a NanoDrop 1000 (Thermo Scientific, software v3.7) at optical densities (OD) 260 and 280 determined nucleic acid purity.

3DNA Array 900 labeling kit (Genisphere, catalog number W500180) was completed for dye reversed cDNA synthesis, isolation and subsequent hybridization of complete genomes. Arrays, were scanned at St. Jude Children's Research Hospital.

Dye reversals of the microarrays were analyzed independently in quadruplicate using the teaching software MAGIC Tool. Tiff files and gene list were loaded using default settings. Spots were located by building an expression file and automated gridding by setting top left/right spots and bottom row, with 19 rows and 22 columns. Under the grid setup window, the default settings were altered to 16 grids, horizontally left to right, vertically top to bottom where spot two is horizontal relative to spot one. Fixed circle segmentation distinguished signal and the log transform of the total signal method was used for gene expression. Gene information was imported to produce the output file. The eight output files were compared to find the 20 most common induced and repressed genes. Utilization of the dye reversal allowed us to rule out false positives.

Gene common names and function were found using the SGD and then compiled into Table 1 grouped by Gene Ontology (GO) functional categories. The gene *YOL154W* (*ZPS1*) stood out as a gene of interest.

Viability Assay

MMY318-1A cultures were grown to log early phase (OD 600 0.25-0.3) in duplicate and serially diluted to concentrations of 1:10, $1:10^2$, $1:10^3$ & $1:10^4$ in sterile water. 2 µL samples of the dilutions were spotted onto SC minimal media plates with 0 µg/mL, 40 µg/mL & 80 µg/mL of KP1019 and a YPD. Plates were incubated at 30˚C until obvious growth of the wildtype strain was observed, then photographed.

Morphology Assay

Cellular and nuclear morphologies were measured using *S. cerevisiae* strains MMY318-1A. These MMY318-1A cultures were grown to log early phase (OD 600 0.25-0.3). The culture was split, and KP1019 was added to half of the culture to a final concentration of 80 µg/ml. After three hours, the treated and untreated cultures were harvested and resuspended in 1X PBS. Formaldehyde was added to the cell suspension to a final concentration of 1.34% to fix the cells. Fixed cells were sonicated for approximately 10 seconds at 4% intensity output (Sonicator Dismembrator Model 100, Fisher Scientific) to disrupt cellular clumps, and placed directly on a slide for budding morphology analysis. Cellular morphology was scored based on the presence or absence of a bud. Buds were considered medium/large if they were larger than approximately one third of the mother cell. At least 100 cells were counted for each sample. Data for three independent technical replicates were collected.

Statistical Analysis

Statistical analysis of the morphologies were carried out in Excel (Microsoft). The average and standard deviation of the three technical replicates were calculated using the average, *AVERAGE*, and sample standard deviation, *STDEV.S*, functions. The standard error was calculated by dividing the returned value from the *STDEV.S* function by the square root, *SQRT*, of the number of samples, *COUNT*, i.e. *STDEV.S/SQRT(COUNT)*. Two times the standard error was calculated by multiplying the returned

value from the standard error by 2. The formulas for the average, sample standard deviation, and standard error are given as follows:

$$\mu = \frac{\sum_{i=1}^{n} x_i}{n}, \quad \sigma = \sqrt{\frac{\sum_{i=1}^{n} (x_i - \bar{x})^2}{n-1}}, \quad SE = \frac{\sigma}{\sqrt{n}}$$

Results

Microarray

Transcriptional analysis via microarray of cells exposed to KP1019 for three hours revealed many induced and repressed genes. To concentrate research efforts, we compiled a gene list of the top twenty most induced and repressed genes (see Table 1). Of the genes repressed, several were related to the cell wall (*PST1*, *SCW11*, *PIR1*, *SUN4*, *EGT2*, *AGA1*, & *SVS1*) and daughter cell separation (*AMN1*, *DSE1*, *CTS1*, *DSE4*, & *DSE3*). A hand full of the repressed genes corresponded to the mother cell (*HO*), transporters (*ITR1*), were zinc related (*ADH4*, *ZPS1*), or related to synthesis (*SAM2*, *INO1*). The remaining repressed genes included ER and mitotic proteins (*WSC4*, *NIS1*). Of the genes induced, several were related to sporulation (*DIT1*, *RIM4*, *YOR336W*), DNA stress response (*UBI4*, *GTT2*, *HUG1*), or were also induced by patulin (*AAD4*, *AAD14*, *NCA3*, *YKL071W*). In addition, RNR (*RNR3*, *RNR4*), Cdc28p substrates (*SIT1*, *YGR035C*), and pheromone (*PRM7*) genes were identified. Transporter (*SNQ2*, *RSB1*), zinc related (*YPR015C*), and NAD related (*BNA2*, *OYE3*) genes were identified. Subsequent gene ontology analysis revealed that near half of genes (~50%) had some direct relation to cellular structure and division, were as 15% of the genes identified in our gene list had unidentified function. The gene *ZPS1* was chosen for further analysis.

Viability assay

Wildtype, *RAD9*Δ, and *ZPS1*Δ strains demonstrated viability at all concentrations when spotted onto a YPD plate (see Fig. 4) thus ensuring all strains had the potential for growth on 0µg/mL, 40µg/mL, & 80µg/mL KP1019 treated SC plates. Both wildtype and *ZPS1*Δ yeast experience dose-dependent reduced viability on the SC plates; further, viability between the two on each SC plate was phenotypically similar. Regardless of the dosage, there was not complete abolishment at any dilution. Comparison of the 0µg/mL and 80µg/mL KP1019 SC plates showed a tentative 15% overall reduction in viability for wildtype and *ZPS1*Δ at all dilutions. On each of the SC plates *RAD9Δ* yeast demonstrated stark reduced viability, even in the absence of KP1019, which was exacerbated in extremity (compared to wildtype) in a dose-dependent manner. KP1019 administered at 40µg/mL and 80µg/mL abolished viability at the $1{:}10^4$ and $1{:}10^1$ dilutions respectively, with a tentative 85% reduction at the $1{:}10^0$ dilution when comparing 0µg/mL and 80µg/mL KP1019 SC plates.

Morphology assay

Cell cycle state of samples of wildtype and *ZPS1Δ* yeast either exposed to KP1019 for three hours or untreated were determine via microscopy to evaluate cellular arrest (see Fig 5). As predicted, wildtype and *ZPS1Δ* demonstrated similar phenotype. Wildtype and *ZPSΔ* untreated and treated yeast were found to have near identical accumulation of large buds (42.67%±3.56 & 49.00%±8.83 untreated respectively; 66.33%±3.56 & 68.00%±5.66 treated respectively). The majority of KP1019 treated *ZPS1Δ* yeast (68.00%±5.66) are found to have large buds, while only about half (49.00%±8.83) of untreated *ZPS1Δ* yeast are found in the same state. Similar is true of wildtype (66.33%±3.56 vs 42.67%±3.56 respectively). Thus deletion of *ZPS1* had no phenotypic affect visible by this assay compared to wildtype, and KP1019 equally caused cellular arrest in both wildtype and *ZPS1Δ*.

Table 1. Gene list of the top twenty induced and repressed genes following 80 µg/mL KP1019 treatment.

Genes altered in the presence of 80µg/mL KP1019					
Induced			Repressed		
Systemic Name	Common Name	Function	Systemic Name	Common Name	Function
YDL038C	*PRM7*	Pheromone-regulated protein; promoter has Gcn4p binding elements;	*YDR055W*	*PST1*	Cell wall protein with putative GPI-attachment site; up-regulated by cell integrity pathway and by cell wall damage via disruption of FKS1;
YDR403W	*DIT1*	Sporulation-specific enzyme required for spore wall maturation;	*YGL028C*	*SCW11*	Cell wall protein with similarity to glucanases; may play a role in conjugation during mating based on its regulation by Ste12p
YHL024W	*RIM4*	Putative RNA-binding protein; required for the expression of early and middle sporulation genes	*YKL164C*	*PIR1*	O-glycosylated protein required for cell wall stability; attached to the cell wall via beta-1,3-glucan; regulated by the cell integrity pathway; mediates mitochondrial translocation of Apn1p
YOR338W		Putative protein of unknown function; required for sporulation in a high-throughput mutant screen;	*YNL066W*	*SUN4*	Cell wall protein related to glucanases; possibly involved in cell wall septation; member of the SUN family;
YGR180C	*RNR4*	Ribonucleotide-diphosphate reductase (RNR) small subunit; rate-limiting step in dNTP synthesis	*YNL327W*	*EGT2*	Glycosylphosphatidylinositol (GPI)-anchored cell wall endoglucanase; required for proper cell separation after cytokinesis;
YIL066C	*RNR3*	Minor isoform of large subunit of ribonucleotide-diphosphate reductase;	*YNR044W*	*AGA1*	Anchorage subunit of a-agglutinin of a-cells; signal for addition of GPI anchor to cell wall, linked to adhesion subunit Aga2p via two disulfide bonds;
YDL243C	*AAD4*	Aryl-alcohol dehydrogenase; oxidative stress response; induced by patulin;	*YPL163C*	*SVS1*	Cell wall and vacuolar protein; required for resistance to vanadate;
YJL116C	*NCA3*	Protein for mitochondrion organization; SUN family ; induced by patulin;	*YBR158W*	*AMN1*	Protein required for daughter cell separation; induced by the Mitotic Exit Network (MEN)
YKL071W		Putative protein of unknown function; induced by patulin, and quinone methide triterpene celastrol; localizes to the cytoplasm	*YER124C*	*DSE1*	Daughter cell-specific protein; may regulate cross-talk between mating and filamentation pathways; deletion affects cell separation after division;
YNL331C	*AAD14*	Putative aryl-alcohol dehydrogenase; mutational analysis has not yet revealed a physiological role;	*YLR286C*	*CTS1*	Endochitinase; required for cell separation after mitosis; transcriptional activation during the G1
YEL065W	*SIT1*	Ferrioxamine B transporter; recognize siderophore-iron chelates; induced by iron deprivation/diauxic shift; potentially phosphorylated by Cdc28p	*YNR067C*	*DSE4*	Daughter cell-specific secreted protein with similarity to glucanases; degrades cell wall from the daughter side causing daughter to separate from mother
YGR035C		Putative protein of unknown function, potential Cdc28p substrate;	*YOR264W*	*DSE3*	Daughter cell-specific protein, may help establish daughter fate; relocalizes from bud neck to cytoplasm upon DNA replication stress
YLL039C	*UBI4*	Ubiquitin; degradation via the ubiquitin-26S proteasome system; essential for stress response; increased by DNA replication stress	*YDL227C*	*HO*	Site-specific endonuclease; generates a ds DNA break; restricted to mother cells in late G1
YLL060C	*GTT2*	Glutathione S-transferase capable of homodimerization; functional overlap with Gtt2p, Grx1p, and Grx2p; increased by DNA replication stress	*YDR497C*	*ITR1*	Myo-inositol transporter; repressed by inositol / choline and derepressed via Ino2p and Ino4p; distribution relative to vacuole increases upon DNA replication stress;
YML058W-A	*HUG1*	Protein involved in the Mec1p-mediated checkpoint pathway; transcription induced by DNA damage; increases to DNA replication stress	*YGL256W*	*ADH4*	Alcohol dehydrogenase isoenzyme type IV; zinc-dependent; transcription induced to zinc deficiency
YPR015C		Putative zinc finger transcription factor; binds DNA in sequence-specific manner; overexpression causes a cell cycle delay or arrest	*YOL154W*	*ZPS1*	Putative GPI-anchored protein; transcription is induced under low-zinc conditions, as mediated by the Zap1p transcription factor, and at alkaline pH
YDR011W	*SNQ2*	Plasma membrane ATP-binding cassette (ABC) transporter; involved in multidrug and SOS resistance	*YDR502C*	*SAM2*	S-adenosylmethionine synthetase; catalyzes transfer of the adenosyl group of ATP to the sulfur atom of methionine;
YOR049C	*RSB1*	Suppressor of sphingoid LCB sensitivity of an LCB-lyase mutation; putative integral membrane transporter or flippase	*YJL153C*	*INO1*	Inositol-3-phosphate synthase; synthesis of inositol phosphates and inositol-containing phospholipids
YJR078W	*BNA2*	Tryptophan 2,3-dioxygenase or indoleamine 2,3-dioxygenase; NAD biosynthesis from tryptophan;	*YHL028W*	*WSC4*	Endoplasmic reticulum (ER) membrane protein; translocation of soluble secretory proteins and insertion of membrane proteins into the ER membrane;
YPL171C	*OYE3*	Conserved NADPH oxidoreductase containing flavin mononucleotide (FMN); potential roles in oxidative stress and apoptosis	*YNL078W*	*NIS1*	Protein localized in the bud neck at G2/M phase; physically interacts with septins; possibly involved in a mitotic signaling network

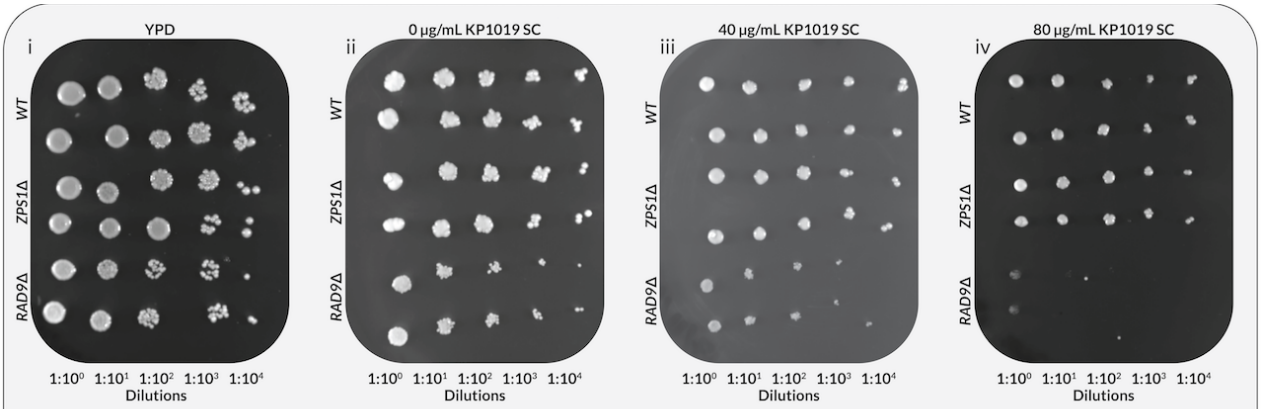

Figure 4: Viability of serially diluted wildtype, *RAD9*Δ, and *ZPS1*Δ yeast with various concentrations of KP1019. i.) Viability on a YPD plate. All strains demonstrate aptitude for growth. **ii.)** Viability on a 0 µg/mL KP1019 SC plate. Growth phenotype for wildtype and *ZPS1*Δ is identical, while *RAD9*Δ demonstrates reduced ability to grow on a nutrient limited plate in the absence of KP1019 **iii.)** Viability on a 40 µg/mL KP1019 SC plate. All strains demonstrate reduced viability compared to the 0 µg/mL KP1019 SC plate with *RAD9*Δ viability abolished at the $1{:}10^4$ dilution **iv.)** Viability on a 80 µg/mL KP1019 SC plate. All strains demonstrate reduced viability compared to the 40 µg/mL KP1019 SC plate with *RAD9*Δ viability abolished at the $1{:}10^1$ dilution. Subtitles describe the plate imaged directly below, x-axes are the dilutions of the strains, and y-axes are the strain type.

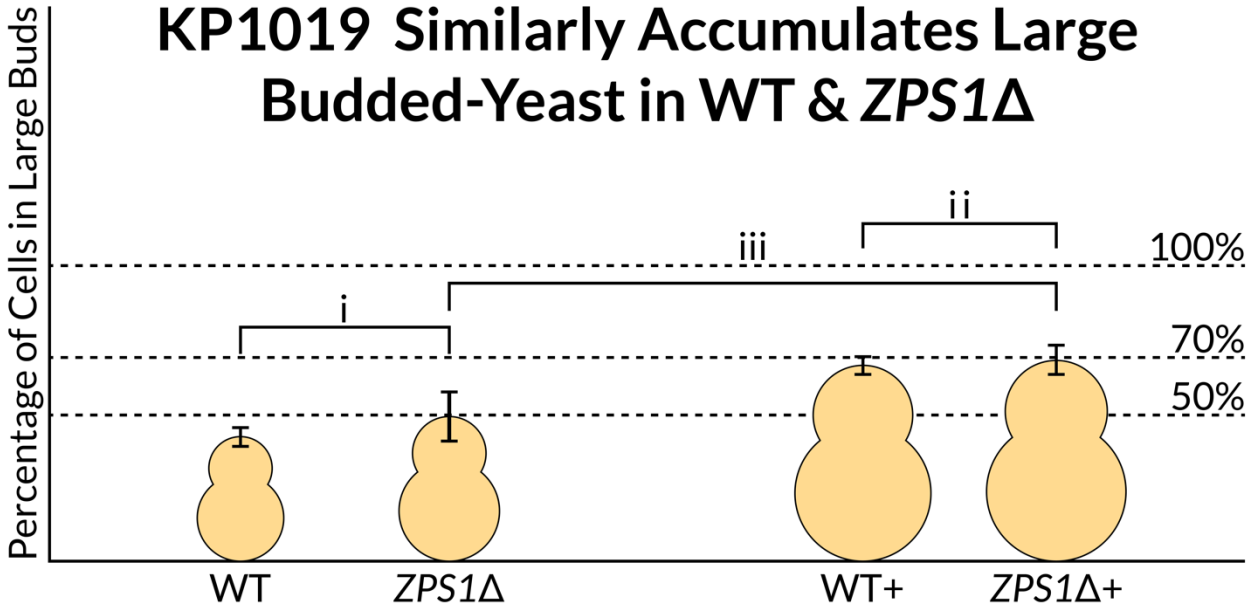

Figure 5: Large budded-yeast accumulation in response to KP1019: **i)** Untreated wildtype and *ZPS1*Δ yeast demonstrate similar accumulation of large buds. **ii)** Treated wildtype and *ZPS1*Δ yeast demonstrate near identical accumulation of large buds. **iii)** Exposure to KP1019 increases cellular arrest in *ZPS1*Δ yeast (phenotypically similar to wildtype. y-axis is the average percentage of yeast observed with large buds, the x-axis is treatment groups. Error bars are 2x standard error.

Discussion

Collective analysis of the microarray, viability, and morphology assays failed to yield a conclusive answer to if zinc starvation via down regulation of *ZPS1* provides KP1019 with the efficacy it has demonstrated against drug resistant cell lines. While initially we predicted a change of DNA check point and anti-apoptosis genes, our microarray analysis instead unveiled many genes involved in structure and division, which are indirectly linked to these events. However, a micro-cluster of genes encoding proteins with zinc cofactors was found. Of interest was the gene *ZPS1* based on research from orthologs and the understanding that the two main transcription factors for drug resistance in yeast, Pdr1 and Pdr3, require zinc (Stevens et al., 2013). As predicted, *ZPS1*Δ did not alter the morphological phenotype in terms of budding index from wildtype. Such adheres to the line of reasoning based on the speculation that *ZPS1* does not play an integral role in DNA repair mechanisms and therefore does little to ameliorate the cellular arrest brought on by KP1019. Further, suppose that the aforesaid speculation is false. As the fungal vacuole can store enough zinc for 8 replication cycles (~200 progeny) and KP1019 exposure was limited to three hours it stands that should zinc be a limiting factor on DNA repair, the repression of *ZPS1* on this time span would be negligible (Eide, 2006; Simm et al., 2007).

This study deliberately chose *not* to look for the mechanism of action for KP1019. Rather, efforts were directed towards elucidating a putative mechanism of efficacy via zinc concentration manipulation. Such manipulation might result from the repression of *ZPS1* - which orthologs suggests a putative zincophore role – repression demonstrated by microarray. Should this hypothesis stand, then purportedly other zinc-dependent modulators may be involved. Intriguingly the putative zinc finger *YPR015C*, was induced. Overexpression of the gene *YPR015C* has been show to cause cellular arrest by evoking a DNA damage checkpoint (Mao et al., 2008; Niu et al., 2008). Zinc starvation, in respect to this transcription factor, may lead to cellular division with defunct DNA: cause of both apoptosis and cancer. However, the yeast genome is known for staggering redundancy and nonessential gene *YPR013C* may have overlapping functionality (Mao et al., 2008). Amongst the other top 20 genes induced or repressed by KP1019 only one other gene directly related to zinc – according to the SGD - was identified: *ADH4*. Yet 53% identical to an iron-ADH of *Zymomonas mobilis*, there remains open debate to *ADH4*'s cofactor (Lyons et al., 2000). Note, that while there is great redundancy in the yeast genome, only *ZPS1* has been indicated via orthologs as a putative zincophore.

Therefore, at first glance, it appears that either *ZPS1*, is a non-redundant gene of critical importance for maintaining zinc homeostasis, or that *ZPS1* has adapted a novel unknown role compared to its orthologs thereby dismissing our hypothesis. However, further analysis of the top 20 lists with YeastRact revealed that 55% of the repressed genes were regulated by the transcription factor Zap1p (p= 0.00021171, data not shown). As outlined in figure 2, the transcription factor possessing seven zinc fingers, Zap1, regulates zinc importers Zrt1, Zrt2, Fet4, as well as putative zincophore Zps1, and Zrt3 which releases zinc from the fungal vacuole (Citiulo et al., 2012; Eide, 2006; Lyons et al., 2000; MacDiarmid et al., 2003; Myers and Myers, 2015; Pagani et al., 2007; Rutherford and Bird, 2004; Simm et al., 2007; Zhao and Eide, 1997). Thereby posing the question whether or not Zap1 is affected by KP1019. Should that be the case, as this unconfirmed coincidence is tantalizing to let us suggest, then KP1019 could disrupt zinc homeostasis on a much grander scale. Further research should investigate a potential connection between KP1019 and Zap1, and the cumulated microarray data might be reconstituted for the purpose of seeing where/if the gene *ZAP1* was altered due to KP1019.

In contrast to our hypothesis, *ZPS1*Δ had no visible affect on the viability assay. While this supports the rejection of our hypothesis, I propose that in actuality, I prematurely hypothesized without the full consideration of the constrictions of the experiment we were assigned to do. Foremost, the timescale on which these experiments took place prevent us from ruling out the effect of the fungal vacuole zinc stores (Citiulo et al., 2012; Eide, 2006; Lyons et al., 2000; MacDiarmid et al., 2003; Myers and Myers, 2015; Pagani et al., 2007; Rutherford and Bird, 2004; Simm et al., 2007; Zhao and Eide, 1997). Further the

medium of use was limited to YPD and SC, both of which contain zinc. Any affect that might have been seen or masked under more appropriate experiments would not allow for us to deduce the affect attributed solely to *ZPS1*Δ and those ameliorated by the remaining members of the zinc homeostasis system (Shet et al., 2011). In addition, orthologs to of Zps1 have been shown to have pH dependent activation and *ZPS1* has demonstrate alkaline-dependent GeneFilter signals (Citiulo et al., 2012; Lamb et al., 2001).

Ideally these two experiments would be carried out once more, with the addendums of a zinc deplete medium, colorimetric assay for intracellular zinc concentrations, periodic introduction to KP1019 and a time series sampling. These four additions allow for the following: analysis in a zinc deplete medium (which would exaggerate and accelerate the time at which affects, if any, were seen by *ZPS1*Δ); quantitative information to intracellular zinc content, which would more definitively confirm or reject our hypothesis; parallel actual application of the drug in clinical trials; and give insight over time to see short/long term affects if they exist. In addition, these experiments should be conduct in tandem to *ZAP1*Δ.

While addressing the limitations due to experimental design is important, and speculating how the hypothesis might still stand true, there remains the glaring issues which are the assumptions underlying the hypothesis. Foremost, the hypothesis is founded on two main assumptions: zinc starvation renders PDR inactive, and Zps1 is critical for preventing zinc starvation. The former can not be addressed without further analysis of both Pdr1's and Pdr3's affinity to zinc as a cofactor. As for the latter, it can not be understated how nearly *all* information regarding Zps1 comes from orthologs. In respect to both the gene and protein *ZPS1* has been largely neglected from *S. cerevisiae* research with the exception of genome-wide studies (Lyons et al., 2000; Pagani et al., 2007). Further, in regards to metallomics, iron has perpetually overshadowed the importance of zinc. The second most common trace metal and present as a cofactor in nearly 10% of proteins in eukaryotes zinc homeostasis remains a rich area of scientific investigation, considering how most of it is uncharted (Citiulo et al., 2012; Eide, 2006; Lyons et al., 2000; MacDiarmid et al., 2003; Myers and Myers, 2015; Pagani et al., 2007; Rutherford and Bird, 2004; Simm et al., 2007; Zhao and Eide, 1997). Only within the last decade have the interactions of the iron and zinc metallomic networks been probed without full understanding of the interface between the two (Courel et al., 2005; Lamb and Mitchell, 2003; Lamb et al., 2001; Pagani et al., 2007; Shanmugam et al., 2012; Yasmin et al., 2009).

The lack of zinc metallomic network research aside, remains the further prodding into the ortholog comparisons. While this zincophore system has been shown to be favorable under evolutionary pressures, and conserved amongst a variety of fungal species it may be also advantageous to dispose of zincophores (Citiulo et al., 2012; Crawford and Wilson, 2015; Wilson, 2015; Wilson et al., 2012). Several hosts for fungal species have developed immune systems apt at recognizing foreign zincophores, and thus such zinc scavenging proteins have become a liability (Citiulo et al., 2012; Crawford and Wilson, 2015; Wilson, 2015; Wilson et al., 2012). Hence posing a plausible explanation as to why Zps1 is found anchored to the cell wall (to limit detection). However, *S. cerevisiae* – baker's yeast - are hardly an invasive fungal species with 92 documented cases as of 2005, thus opening up the argument that a zincophore system, such as that found in *C. albicans*, is not necessary for *S. cerevisiae* (Enache-Angoulvant and Hennequin, 2005). Contradictory, however, is that clinically the infection of *S. cerevisiae* and candidiasis are indistinguishable (Enache-Angoulvant and Hennequin, 2005). Therefore, given accessible data and this experiment, one can not deduce the function or likelihood of *ZPS1* having relevant zincophore functionality. More in-depth discussion of *ZPS1* as a zincophore is carried out in the supplemental material section.

In conclusion, while our hypothesis is theoretically both interesting and plausible, the set of experiments carried out here were not able to definitively rule one way or the other. At most, the only outcome which can be concluded is that the deletion of *ZPS1* does not exacerbate the mechanism of action of a single dose of KP1019 on a short time scale.

Supplemental Material

Structural Analysis

Models of proteins were predicted, analyzed and docked using Phyre2, RaptorX JMol, DLigandSite, and ZDock. Protein images were generated using Protean3D (DNASTAR) and JMol. Protean3D was used for model alignment The informal evaluation of "successful" docking resulted by transforming ZDock output into a set of coordinate points for the top 500 docked models and then analyzed for nearest neighbor cluster in Weka. (Hall et al.; Källberg et al., 2012; Kelley et al., 2015; Pierce et al., 2014; Wass et al., 2010; JMol; Protean3D™)

About Protein Structure Prediction

Both Phyre2 and RaptorX use homology template based modeling. In regards to accuracy, software use is largely arbitrary. Phyre2, however, is within the top 6 out of 55 other programs, where the five above ranking software had an average of 2.8% improvement (a 1% improvement is approximately 2 extra residues within 4.5Å of the native structure). Homology based modeling is much stronger in terms of accuracy than ab initio – taking into account evolutionary related and functionally conserved structures.

About Docking Analysis

This "informal" evaluation, still yields useful information of docking as the ZDock algorithm considers the pdb files static. Therefore, a high density of models in a single neighborhood can be thought of as a crude representation of dynamic nature of protein interactions.

Structural Results

The majority (>66%) of the following proteins were predicted with high confidence, Zps1, Zrt1, Zrt2, and Fet4 (see figure 6). Zps1 was modeled in Phyre2, where 67% of the protein conformed to homology matches with 100% confidence ($p = 4.58x10^{-7}$). Note, confidence here does not reflect the expected accuracy of the model, although these two notions are highly related. The third of the protein not predicted by Phyre2 was deemed unstructured. Alignment was confirmed with the predicted structure from RaptorX in Protean3D (data not shown). Phyre2's homology based algorithm did not construct decent models for membrane bound proteins Zrt1, Zrt2, and Fet4. These were modeled in RaptorX. The difference in model results most likely is emergent of the database of templates from which these servers draw. All of the residues where modeled for Zrt1 ($p = 7.53x10^{-5}$), Zrt2 ($p = 4.58x10^{-5}$) and Fet4 ($p = 6.40x10^{-5}$) which pass the threshold for significance of confidence for proteins composed largely of alpha helices.

Docking Results

DLigandSite identified a prominent site within the Zps1 model for zinc binding utilizing residues His186, His190, Glu202, and Thr225. Both Zrt1 and Zrt2 (figure 6.ii) demonstrated a main cluster with a quasi-normal distribution about the cluster's center. Fet4 demonstrated three clusters in a diagonal orbit about the transmembrane helices.

Structural and Docking Discussion

Homology based modeling from Phyre2 and RaptorX demonstrated that although transmembrane proteins are notorious for their difficulty of structure resolution by traditional means, current information allows for sufficient approximations of these structures. Further, the templates from which these models were built, reflected functional or structural homology with metalloproteins. Importantly, the Zps1 structure has only one predicted binding site for zinc. This is a stark contrast to its *C. albicans* ortholog, which can bind up to 3 zinc atoms, thereby bringing into question Zps1's putative zincophore function.

While the nature of this study prevented further examination of Zps1 and its function, we hypothesis that should Zps1 indeed be a zincophore, then Zps1 will dock in some fashion to at least one, if not more, of the main zinc importers. Indeed, Zps1 does "dock" to the homology based predicted structures of Zrt1, Zrt2, and Fet4. However, these results *must* be taken with some skepticism. Foremost, one may be concerned of the accuracy of predicted docking to a transmembrane protein, given that some of that protein is not accessible. However, recall that Zps1 membrane bound, allowing for a closer interaction, but not necessarily to transmembrane parts. Second, the orientation of these predicted models are completely unknown. To that end, while a cluster might represent a putative binding site, the "site" at which it binds may very well be intracellular. Similar

to the above concern, ZDock's docking methodology pay no mind to orientation of the "ligand." Perhaps ZDock correctly predicted that Zps1 bound to Zrt1 at a physiological possible site – however that docking might only occur when Zps1 is oriented perpendicularly to how it is found endogenously. The accuracy of these binding site predictions can be improved remarkably by constraining the receptors and Zps1 to a membrane to determine orientation. As for now, it can be noted that Zps1 putatively interacts with zinc importers Zrt1, Zrt2, and Fet4. Of further concern, is that such docking was conducted on an "unloaded" Zps1, in that Zps1 did not have zinc bound when docked. In relation to the primary discussion, the structural information derived here lends favor to the idea of Zps1 being a zincophore, especially the putative interactions with main zinc importers. Given that over 50% of the repressed genes in our top 20 repressed list had Zap1p as a transcription factor, these so far only theoretical coincidences are tempting to not ignore. Further research, as suggested above, may included *ZAP1*Δ and zinc concentration analyses.

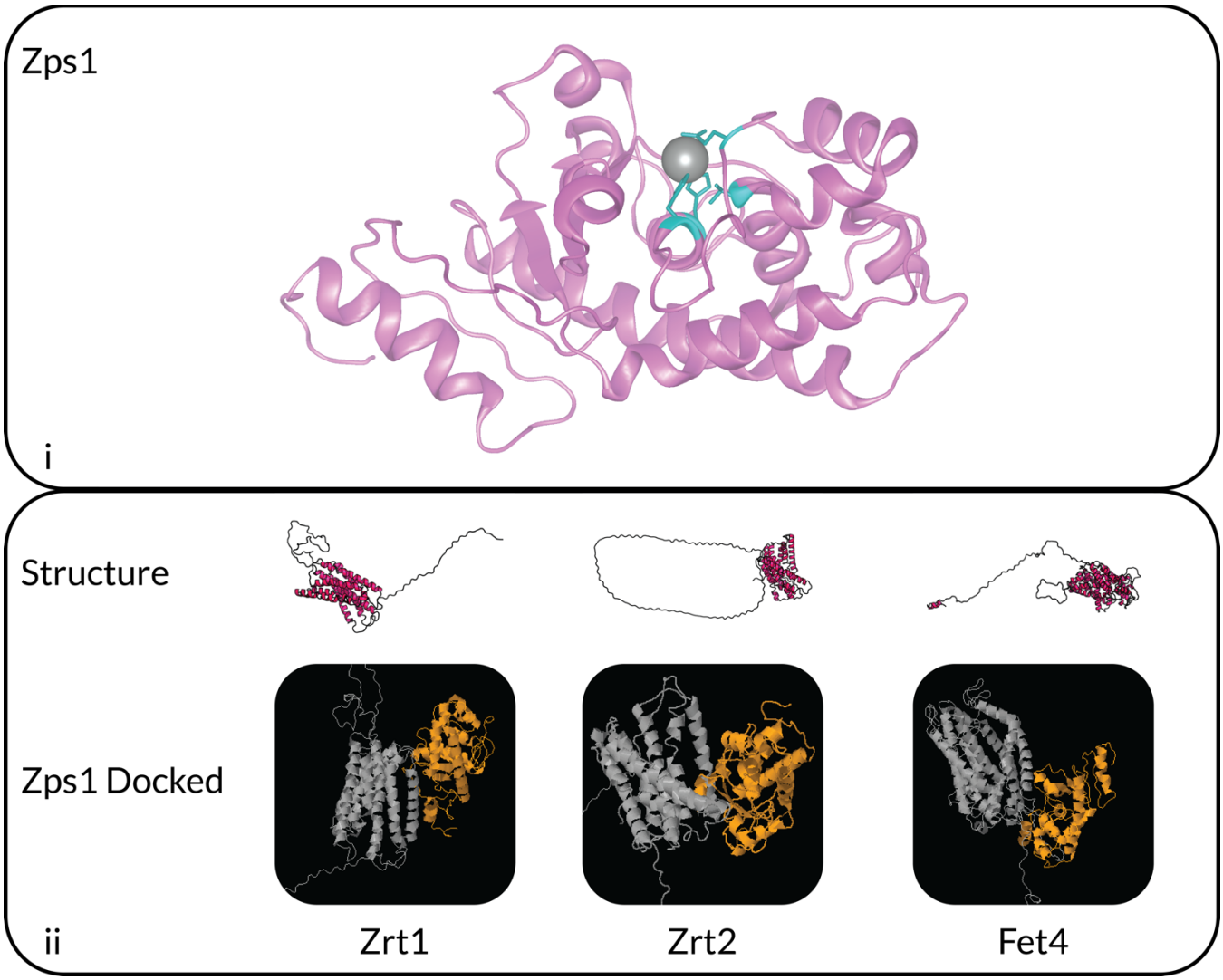

Figure 6. Structural and docking results of zinc related proteins. i.) Model of the Zps1 with zinc atom. Binding site residues highlighted in blue. **ii.)** Models of Zrt1, Zrt2 and Fet4 above. Models of Zrt1, Zrt2 and Fet4 (gray) docked with Zps1 (orange) below.

Works Cited

1. Antonarakis, E.S., and Emadi, A. (2010). Ruthenium-based chemotherapeutics: are they ready for prime time? Cancer Chemother. Pharmacol. *66*, 1–9.

2. Baitalik, S., and Adhikary, B. (1997). Heterochelates of ruthenium(II): electrochemistry, absorption spectra, and luminescence properties. Polyhedron *16*, 4073–4080.

3. Chakravarty, J., and Bhattacharya, S. (1996). Ruthenium phenolates, synthesis, characterization and electron-transfer properties of some salicylaldiminato and 2-(arylazo)phenolato complexes of ruthenium. Polyhedron *15*, 1047–1055.

4. Citiulo, F., Jacobsen, I.D., Miramón, P., Schild, L., Brunke, S., Zipfel, P., Brock, M., Hube, B., and Wilson, D. (2012). Candida albicans Scavenges Host Zinc via Pra1 during Endothelial Invasion. PLoS Pathog *8*, e1002777.

5. Courel, M., Lallet, S., Camadro, J.-M., and Blaiseau, P.-L. (2005). Direct Activation of Genes Involved in Intracellular Iron Use by the Yeast Iron-Responsive Transcription Factor Aft2 without Its Paralog Aft1. Mol. Cell. Biol. *25*, 6760–6771.

6. Crawford, A., and Wilson, D. (2015). Essential metals at the host–pathogen interface: nutritional immunity and micronutrient assimilation by human fungal pathogens. FEMS Yeast Res. *15*, fov071.

7. Eide, D.J. (2006). Zinc transporters and the cellular trafficking of zinc. Biochim. Biophys. Acta BBA - Mol. Cell Res. *1763*, 711–722.

8. Enache-Angoulvant, A., and Hennequin, C. (2005). Invasive Saccharomyces Infection: A Comprehensive Review. Clin. Infect. Dis. *41*, 1559–1568.

9. Foury, F. (1997). Human genetic diseases: a cross-talk between man and yeast. Gene *195*, 1–10.

10. Goffeau, A., Barrell, B.G., Bussey, H., Davis, R.W., Dujon, B., Feldmann, H., Galibert, F., Hoheisel, J.D., Jacq, C., Johnston, M., et al. (1996). Life with 6000 genes. Science *274*, 546, 563–567.

11. Hall, M., Frank, E., Holmes, G., Pfahringer, B., Reutemann, P., and Witten, I. The WEKA Data Mining Software: An Update. SIGKDD Explor. *11*, 10–18.

12. Hartinger, C.G., Zorbas-Seifried, S., Jakupec, M.A., Kynast, B., Zorbas, H., and Keppler, B.K. (2006). From bench to bedside – preclinical and early clinical development of the anticancer agent indazolium trans-[tetrachlorobis(1H-indazole)ruthenate(III)] (KP1019 or FFC14A). J. Inorg. Biochem. *100*, 891–904.

13. Heffeter, P., Pongratz, M., Steiner, E., Chiba, P., Jakupec, M.A., Elbling, L., Marian, B., Körner, W., Sevelda, F., Micksche, M., et al. (2005). Intrinsic and acquired forms of resistance against the anticancer ruthenium compound KP1019 [indazolium trans-[tetrachlorobis(1H-indazole)ruthenate (III)] (FFC14A). J. Pharmacol. Exp. Ther. *312*, 281–289.

14. Heffeter, P., Jungwirth, U., Jakupec, M., Hartinger, C., Galanski, M., Elbling, L., Micksche, M., Keppler, B., and Berger, W. (2008). Resistance against novel anticancer metal compounds: differences and similarities. Drug Resist. Updat. Rev. Comment. Antimicrob. Anticancer Chemother. *11*, 1–16.

15. Källberg, M., Wang, H., Wang, S., Peng, J., Wang, Z., Lu, H., and Xu, J. (2012). Template-based protein structure modeling using the RaptorX web server. Nat. Protoc. *7*, 1511–1522.

16. Kapitza, S., Jakupec, M.A., Uhl, M., Keppler, B.K., and Marian, B. (2005a). The heterocyclic ruthenium(III) complex KP1019 (FFC14A) causes DNA damage and oxidative stress in colorectal tumor cells. Cancer Lett. *226*, 115–121.

17. Kapitza, S., Pongratz, M., Jakupec, M.A., Heffeter, P., Berger, W., Lackinger, L., Keppler, B.K., and Marian, B. (2005b). Heterocyclic complexes of ruthenium(III) induce apoptosis in colorectal carcinoma cells. J. Cancer Res. Clin. Oncol. *131*, 101–110.

18. Kelley, L.A., Mezulis, S., Yates, C.M., Wass, M.N., and Sternberg, M.J.E. (2015). The Phyre2 web portal for protein modeling, prediction and analysis. Nat. Protoc. *10*, 845–858.

19. Kratz, F., and Messori, L. (1993). Spectral characterization of ruthenium (III) transferrin. J. Inorg. Biochem. *49*, 79–82.

20. Lamb, T.M., and Mitchell, A.P. (2003). The Transcription Factor Rim101p Governs Ion Tolerance and Cell Differentiation by Direct Repression of the Regulatory Genes NRG1 and SMP1 in Saccharomyces cerevisiae. Mol. Cell. Biol. *23*, 677–686.

21. Lamb, T.M., Xu, W., Diamond, A., and Mitchell, A.P. (2001). Alkaline Response Genes of Saccharomyces cerevisiaeand Their Relationship to the RIM101 Pathway. J. Biol. Chem. *276*, 1850–1856.

22. Lyons, T.J., Gasch, A.P., Gaither, L.A., Botstein, D., Brown, P.O., and Eide, D.J. (2000). Genome-wide characterization of the Zap1p zinc-responsive regulon in yeast. Proc. Natl. Acad. Sci. *97*, 7957–7962.

23. MacDiarmid, C.W., Milanick, M.A., and Eide, D.J. (2003). Induction of the ZRC1 Metal Tolerance Gene in Zinc-limited Yeast Confers Resistance to Zinc Shock. J. Biol. Chem. *278*, 15065–15072.

24. Mao, J., Habib, T., Shenwu, M., Kang, B., Allen, W., Robertson, L., Yang, J.Y., and Deng, Y. (2008). Transcriptome profiling of Saccharomyces cerevisiae mutants lacking C2H2 zinc finger proteins. BMC Genomics *9*, S14.

25. Menacho-Márquez, M., and Murguía, J.R. (2007). Yeast on drugs: Saccharomyces cerevisiae as a tool for anticancer drug research. Clin. Transl. Oncol. *9*, 221–228.

26. Myers, S.A., and Myers, S.A. (2015). Zinc Transporters and Zinc Signaling: New Insights into Their Role in Type 2 Diabetes, Zinc Transporters and Zinc Signaling: New Insights into Their Role in Type 2 Diabetes. Int. J. Endocrinol. Int. J. Endocrinol. *2015*, *2015*, e167503.

27. Niu, W., Li, Z., Zhan, W., Iyer, V.R., and Marcotte, E.M. (2008). Mechanisms of Cell Cycle Control Revealed by a Systematic and Quantitative Overexpression Screen in S. cerevisiae. PLoS Genet *4*, e1000120.

28. Pagani, M.A., Casamayor, A., Serrano, R., Atrian, S., and Ariño, J. (2007). Disruption of iron homeostasis in Saccharomyces cerevisiae by high zinc levels: a genome-wide study. Mol. Microbiol. *65*, 521–537.

29. Pierce, B.G., Wiehe, K., Hwang, H., Kim, B.-H., Vreven, T., and Weng, Z. (2014). ZDOCK server: interactive docking prediction of protein-protein complexes and symmetric multimers. Bioinforma. Oxf. Engl. *30*, 1771–1773.

30. Rutherford, J.C., and Bird, A.J. (2004). Metal-Responsive Transcription Factors That Regulate Iron, Zinc, and Copper Homeostasis in Eukaryotic Cells. Eukaryot. Cell *3*, 1–13.

31. Sava, G., and Bergamo, A. (2000). Ruthenium-based compounds and tumour growth control (review). Int. J. Oncol. *17*, 353–365.

32. Sava, G., Zorzet, S., Giraldi, T., Mestroni, G., and Zassinovich, G. (1984). Antineoplastic activity and toxicity of an organometallic complex of ruthenium(II) in comparison with cis-PDD in mice bearing solid malignant neoplasms. Eur. J. Cancer Clin. Oncol. *20*, 841–847.

33. Schluga, P., Hartinger, C.G., Egger, A., Reisner, E., Galanski, M., Jakupec, M.A., and Keppler, B.K. (2006). Redox behavior of tumor-inhibiting ruthenium(III) complexes and effects of physiological reductants on their binding to GMP. Dalton Trans. Camb. Engl. 2003 1796–1802.

34. Shanmugam, V., Tsednee, M., and Yeh, K.-C. (2012). ZINC TOLERANCE INDUCED BY IRON 1 reveals the importance of glutathione in the cross-homeostasis between zinc and iron in Arabidopsis thaliana. TPJ Plant J. *69*, 1006–1017.

35. Shet, A., Patil, L., Hombalimath, V., Yaraguppi, D., and Udapudi, B. (2011). Enrichment of Saccharomyces cerevisiae with zinc and their impact on cell growth. Biotechnol. Bioinforma. Bioeng. *1*, 523:527.

36. Simm, C., Lahner, B., Salt, D., LeFurgey, A., Ingram, P., Yandell, B., and Eide, D.J. (2007). Saccharomyces cerevisiae Vacuole in Zinc Storage and Intracellular Zinc Distribution. Eukaryot. Cell *6*, 1166–1177.

37. Stevens, S.K., Strehle, A.P., Miller, R.L., Gammons, S.H., Hoffman, K.J., McCarty, J.T., Miller, M.E., Stultz, L.K., and Hanson, P.K. (2013). The Anticancer Ruthenium Complex KP1019 Induces DNA Damage, Leading to Cell Cycle Delay and Cell Death in Saccharomyces cerevisiae. Mol. Pharmacol. *83*, 225–234.

38. Wass, M.N., Kelley, L.A., and Sternberg, M.J.E. (2010). 3DLigandSite: predicting ligand-binding sites using similar structures. Nucleic Acids Res. *38*, W469–W473.

39. Weinberg, R.A. (1996). How cancer arises. Sci. Am. *275*, 62–70.

40. Wilson, D. (2015). An evolutionary perspective on zinc uptake by human fungal pathogens. Met. Integr. Biometal Sci. *7*, 979–985.

41. Wilson, D., Citiulo, F., and Hube, B. (2012). Zinc Exploitation by Pathogenic Fungi. PLoS Pathog. *8*.

42. Yasmin, S., Abt, B., Schrettl, M., Moussa, T.A.A., Werner, E.R., and Haas, H. (2009). The interplay between iron and zinc metabolism in Aspergillus fumigatus. Fungal Genet. Biol. FG B *46*, 707–713.

43. Zhao, H., and Eide, D.J. (1997). Zap1p, a metalloregulatory protein involved in zinc-responsive transcriptional regulation in Saccharomyces cerevisiae. Mol. Cell. Biol. *17*, 5044–5052.

44. (2004). Microarrays: Chipping Away at the Mysteries of Science and Medicine. NCBI.

45. Saccharomyces Genome Database.

46. Jmol: an open-source Java viewer for chemical structures in 3D.

47. Protean3D (Madison, WI: DNASTAR).